metals

MDPI

Article

Characterization of Influences of Steel-Aluminum Dissimilar Joints with Intermediate Zinc Layer

Tobias Bick, Verena Heuler, Kai Treutler * and Volker Wesling

Institute of Welding and Machining – Clausthal University of Technology, 38678 Clausthal-Zellerfeld, Germany; tobias.bick@tu-clausthal.de (T.B.); verena.heuler@tu-clausthal.de (V.H.); office@isaf.tu-clausthal.de (V.W.)

* Correspondence: treutler@isaf.tu-clausthal.de; Tel.: +49-5323-72-2110

Received: 19 February 2020; Accepted: 25 March 2020; Published: 27 March 2020

Abstract: Brittle intermetallic phases are formed when steel and aluminum are joined. Therefore, it is difficult to use this combination of materials when applying the multimaterial design in the construction of load-adapted and weight-adapted structures. In order to largely avoid the formation of these brittle phases, joining processes based on diffusion processes, such as composite forging, depict a good solution approach. The materials are joined in a solid state. Furthermore, zinc additives are used to create the joint. Zinc forms a compound with both steel and aluminum without the formation of brittle phases. By combining the composite forging process with zinc additives, strength values of 26 N/mm^2 can be reached. This is higher, in comparison to former investigations of resistance spot welded and clinched joints. The joint properties depend on the composition of the zinc interlayer. Small amounts of magnesium in the zinc interlayer affected the strength and ductility values. While the strength decreased by about 30% in contrast to the zinc layer without magnesium, the ductility increased by 60%. This effect was probably due to the metallurgical impact of the alloying elements on phase formation, as could be shown by energy dispersive X-ray spectroscopy (EDX) analyses of the joint zones. Thereby, it was shown that the brittle intermetallic phases are located only in small areas.

Keywords: diffusion bonding; intermetallics; hybrid joints; steel; aluminum

1. Introduction

Lightweight constructions in multimaterial designs significantly contribute to saving weight and resources. The use of high-strength and ultrahigh-strength steel in combination with light metals, such as aluminum and magnesium, allows for the production of load-adapted and weight-optimized car bodies. To protect the steel from corrosion in the surrounding atmosphere, the sheets are often coated with a zinc layer. In addition to this pure zinc layer, the state-of-the-art is to also use a zinc layer which contains magnesium [1]. However, this construction method requires joining technology concepts to produce load-compatible joints out of the respective metallic materials. Particularly in the compound of aluminum and steel, brittle intermetallic iron-aluminum (Fe-Al) phases are usually formed during metallic continuity, especially because of a thermal joining process, due to the molten state [2,3]. Li et al. analyzed and calculated the intermetallic compound properties and their effects on steel-aluminum laser welding and the mechanical properties of the joints [4]. Depending on the composition, the hardness values of these intermediate compounds were up to 1100 HV0.0005, which significantly reduced the mechanical properties of the compound [2,5]. Therefore, a large number of investigations have been carried out to reduce phase growth or prevent the formation of phases [6–8].

Goldmann et al., as well as Leuschen, investigated the behavior of phase formation and the microstructure morphology during the resistance spot welding of a steel-aluminum combination under process-related aspects [3,9,10]. They showed that short welding times and high welding currents led to low phase growth and relatively good strength properties. Pereira et al. worked

on optimal laser welding parameters for dissimilar-metals laser welding, based on mechanical and microstructure investigations [11]. Guan et al. further analyzed the effects of laser welding parameters on the mechanical properties of aluminum-steel joints [12]. Additionally, Lu et al. studied a laser-metal inert gas hybrid welding process and its parameters to improve the weld formation in steel-aluminum joints [13]. Furthermore, Matsuda et al. analyzed the impacts of various process parameters on the mechanical properties and the formation of intermetallic compounds in a high-frequency linear friction welding process [14]. Beyond that, Mrzljak et al. used magnetic pulse welding in order to optimize the process parameters for joining steel to aluminum [15]. In addition to process modification, the influence of filler and coating materials was also investigated in the literature [16–19]. For example, a zinc coating on the steel sheets led to improved strength properties during resistance spot welding compared to uncoated sheets, as Eichhorn et al. showed [20].

Since the formation of phases is supported when the materials are brought into the molten state, alternative hybrid joining methods have been used [21–24]. Girard et al. showed a reduced formation of intermetallic phases during friction stir welding when the mixing of the materials is minimized [25]. However, in no joining process could the formation of intermediate phases during metallic continuity joining be avoided. Therefore, a recommendation was made to keep the characteristic phase seam smaller than 10 µm [26]. A further approach is compound forging. In this process, hot forming is used to create form, force and/or metallic continuity joints [27–31]. The joining partners are not converted into molten state during the process, and only a slight formation of intermetallic Fe-Al phases occurs. By applying an additional zinc layer on the aluminum base material, a continuous metallic joint can be produced that contains only a small amount of intermetallic phases in the zinc layer [32,33]. In addition, the coating of aluminum with zinc destroys the characteristic oxide layer. This results in a better bond between the material surfaces [34] Since the zinc layer significantly contributes to the formation of the joint, this process is referred to as hybrid composite forging.

This publication investigates the influence of the element magnesium in the zinc layer of the steel sheet on phase formation and on the strength and ductility properties. Within these tests, the aluminum bolts were first provided with a zinc coating by hot-dip galvanizing. The galvanized aluminum bolts were then joined under pressure and temperature with the steel sheets. The chemical composition of the resulting phases in the zinc interlayer was determined by an EDX analysis. On the basis of the compositions, an estimating classification was made with reference to the corresponding three-component systems.

2. Materials and Experimental Procedure

Solid cylindrical aluminum bolts made of AlMg4.5Mn, and steel sheets of quality DX54 with zinc coatings of different chemical compositions were used for the production and investigation of dissimilar joints. A pure zinc layer with a thickness of 7 µm to 10 µm and a layer with a content of magnesium up to 2 wt.-% were used in this investigation. Figure 1 shows a schematic illustration of a dissimilar joint specimen with the zinc coated steel sheet on the upper side and aluminum bolt below. The thickness of the steel sheet was about 1 mm and the effective diameter of the bolt was about 10 mm. The characteristic values of the test materials are listed in Table 1. The chemical composition of the aluminum material is listed in Table 2.

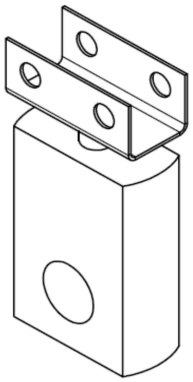

Figure 1. Schematic illustration of the specimen geometry.

Table 1. Mechanical properties of the base materials.

Material	Tensile Strength	Yield Strength	Elastic Modulus	Elongation at Break	Yield Point
AlMg4.5Mn	329 MPa	223 MPa	92,400 MPa	14.36%	328 MPa
DX54	260 MPa	120 MPa	210,000 MPa	36%	-

Table 2. Chemical compositions of used materials (wt.-%).

AlMg4.5Mn							
Al	Mg	Mn	Fe	Si	Cr	Zn	Cu
94.3	4.489	0.515	0.3042	0.1555	0.0796	0.0470	0.0403
DX54							
Fe	C	Si	Mn	P	S	Ti	Al
99.47	0.011	0.029	0.113	0.012	0.0082	0.094	0.062

In general, this aluminum alloy has good weldability, as well as corrosion resistance, and is therefore frequently used in apparatus, container, and vehicle construction. Due to its good low-temperature properties and resistance to seawater, this alloy is also used in shipbuilding. The DX54 is a hot-dip galvanized deep-drawing steel that is mainly used for car body construction [32,33].

The solid aluminum parts were coated with zinc before the joining process. This prevented direct contact of the two base materials during the joining process. An electrolytically deposited layer (thickness < 7 µm) did not prove to be useful during prior investigations, as it broke up during the joining process, leading to direct contact between aluminum and steel [32,33]. This resulted in the formation of brittle intermetallic phases and thereby did not create a sufficiently strong material joint. For this reason, hot-dip galvanizing was used. However, since aluminum and zinc represent a system with a low-melting eutectic (Figure 2), the composition of the molten zinc had to be adjusted by wet chemical means in order to prevent melting of the aluminum sample. Figure 2 shows the microstructures of the hypoeutectic, eutectic, and hypereutectic compositions in metallographic sections. According to Figure 2, the composition of the molten zinc used for zinc coating was located on the left side of the eutectic at a solidification temperature of 387 °C. It contained 83% zinc and 17% aluminum. The samples of the aluminum base material were dipped into the molten zinc for 20 min at 420 °C in a furnace. The diffusion process led to the dissolution of the oxide layer and, further, to the formation of a zinc layer with a thickness of up to 150 µm on the aluminum specimen [32,33,35].

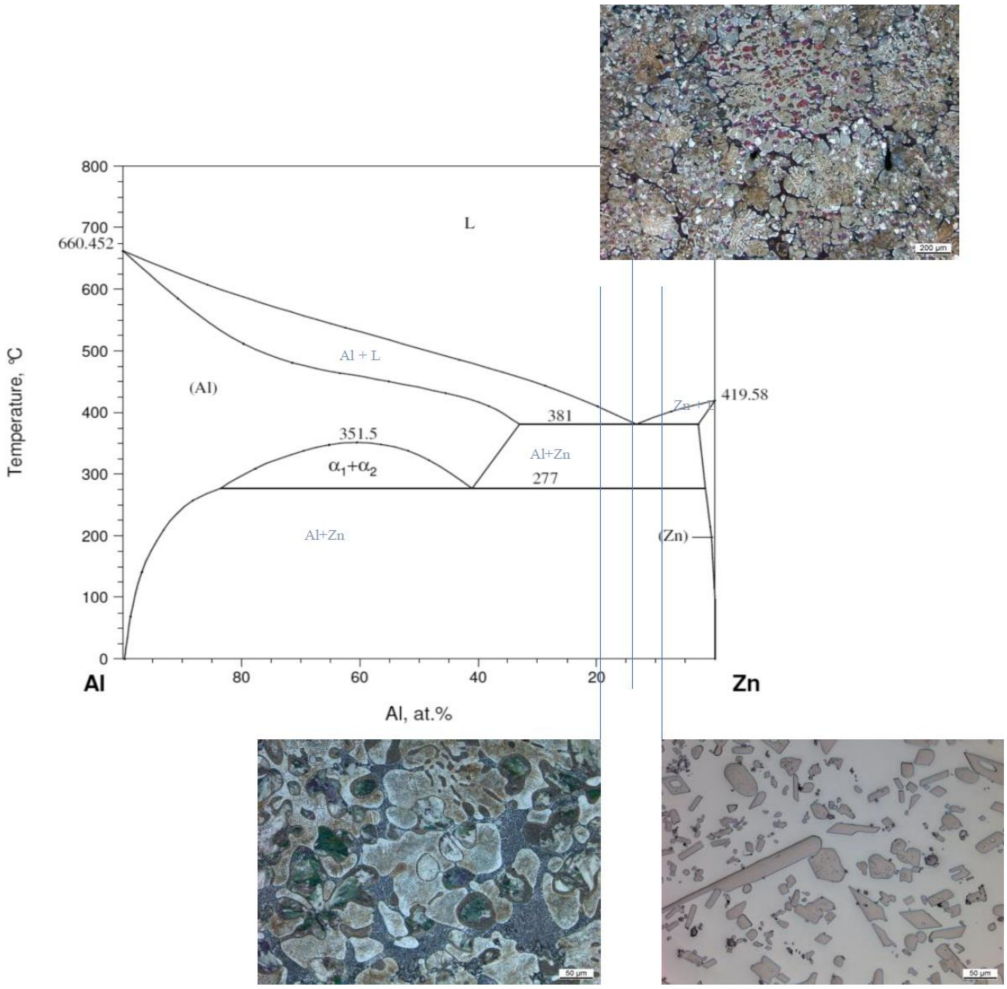

Figure 2. Al-Zn phase diagram [10].

The coated bolts were then joined to the steel sheets in a test stand for hot tensile and compression tests as shown in Figure 3.

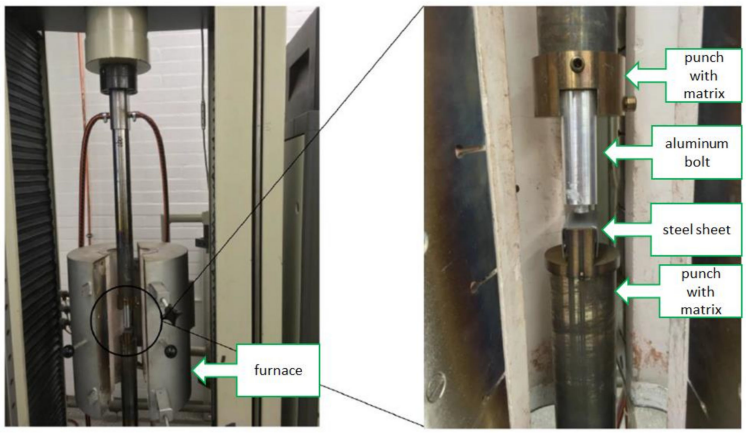

Figure 3. Test set-up for the production of metallic continuous joints.

The steel and aluminum parts of the samples were placed in the corresponding matrices (Figure 3) and preheated in the furnace for 20 min. The joining process was then carried out according to the specified process parameters of sample temperature, punch force, and punch speed. The courses of the

punch force and displacement, as well as the surface temperature of the aluminum bolt, are shown in Figure 4. These tests were model tests of a forging process with reduced speed. The temperature curve showed that the zinc layer on the aluminum did not melt during the joining process (Ts(zinc) > 387 °C). Thus, the diffusion process led to the formation of a firmly bonded joint. Explicit detailed investigations of the processes in the joining zone are still pending. Therefore, no statement on the exact classification of the joining process can be made at the present.

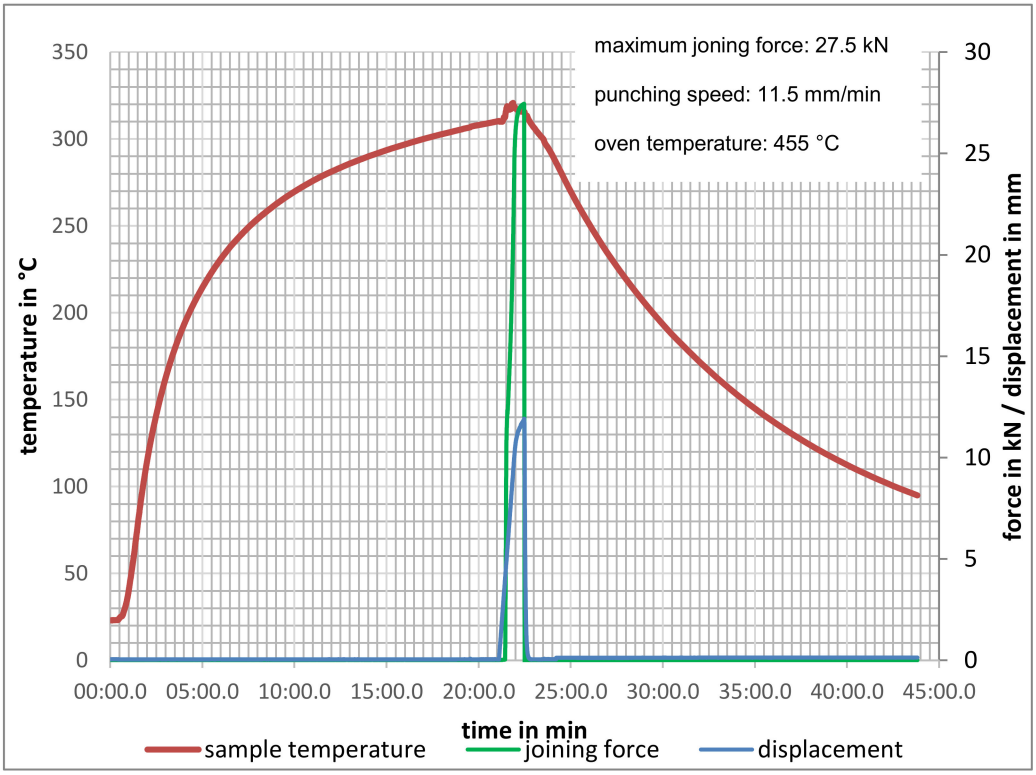

Figure 4. Force, displacement, and temperature graphs of the joining process.

3. Phase Classification and Results of Tensile Testing

Figure 5 shows the firmly bonded joint with a pure zinc layer on the steel sheet in the scanning electron microscope at 250× magnification. Furthermore, it shows the corresponding EDX analysis listed in tabular form. The chemical compositions in the measuring points were categorized to the corresponding phases according to the isothermal section in the ternary system Fe-Al-Zn at 330 °C (Figure 6) [36]. The composition in the measuring points EDX 01, 02, and 10 corresponded to the base materials. The material in the measuring points EDX 03, 05 and 08 consisted of more than 98 at.-% Zn, which probably indicated zinc mixed crystals (Zn).

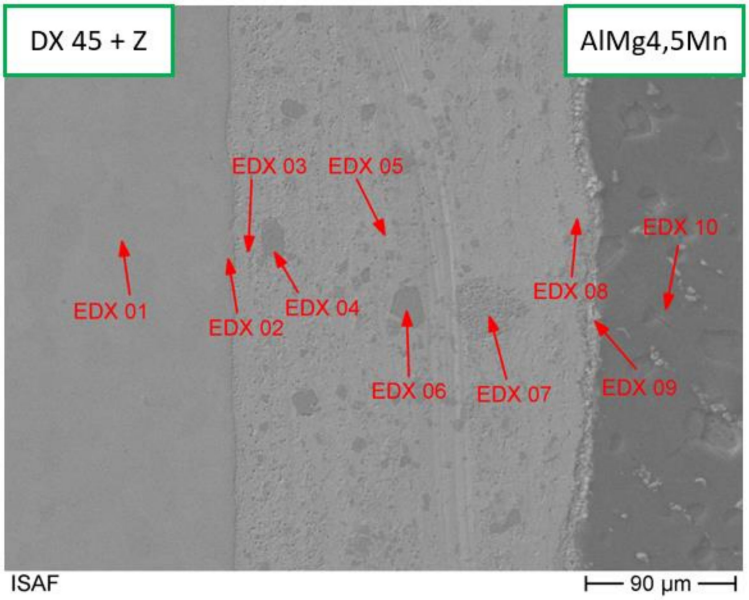

EDX-Point:	Fe (at.%)	Al (at.%)	Zn (at.%)	Mg (at.%)	Si (at.%)	Phases
01	DX54D					
02	DX54D					
03	-	0.91	98.32	-	0.77	(Zn)
04	-	60.21	36.23	-	3.56	(Al‘) + (Al“) + Fe4Al13
05	-	1.08	98.26	-	0.65	(Zn)
06	8.26	26.9	64.84	-	-	(Al‘) + (Zn) + Fe_4Al_{13}
07	37.71	54.27	7.45	-	0.57	n. b.
08	-	1.11	98.14	-	0.75	(Zn)
09	7.13	30.73	56.57	2.62	2.95	(Al‘) + (Zn‘) + Fe_4Al_{13}
10	AlMg4.5Mn					

Figure 5. EDX analysis of the generated compound with pure zinc layer.

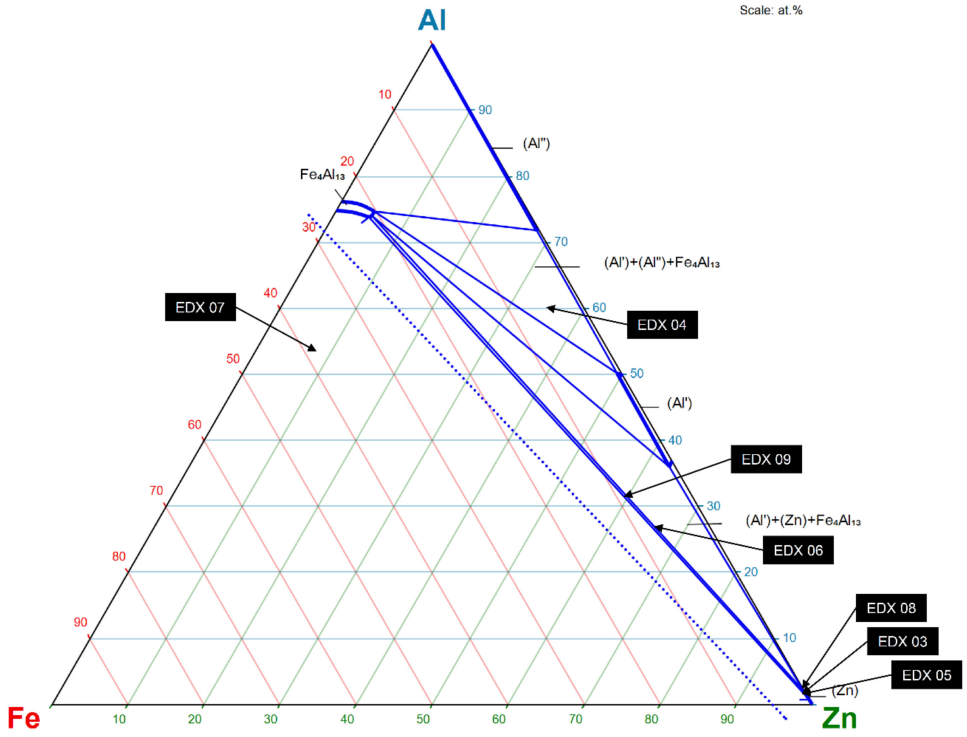

Figure 6. Isothermal section of the ternary system Al-Fe-Zn at 330 °C with EDX points. [25].

The measuring point EDX 07 could not clearly be categorized based on the isothermal section shown. However, the isothermal section at 330 °C suggested that this measuring point was a crystal mixture of (α-Fe), $FeZn_{10}$ and Fe_2Al_5. According to the classification, the points EDX 04, 06 and 09 suggested the brittle intermetallic phase Fe_4Al_{13}, as well as zinc (Zn) and aluminum (Al) mixed crystals. The high silicon content of the EDX analyses indicated precipitates containing silicon, as the silicon content of the base materials was significantly lower. In order to confirm this, further investigations are currently being carried out for phase analysis using XRD.

Therefore, the intermediate layer of the compound probably consisted mainly of zinc mixed crystals. This means that mainly Al-Zn mixed crystals of different composition and the brittle Fe_4Al_{13} phase were precipitated. The proportion of brittle intermetallic Fe-Al phases was very low and they appeared only locally. This means that there was no continuous phase seam, as is usually the case. Nevertheless, the Fe_4Al_{13} phase belonged to the hard and brittle metastable phases. Thus, the zinc interlayer largely prevented direct contact between Fe and Al, resulting in the formation of only a few dispersed intermetallic Fe-Al phases.

In comparison to this, Figure 7 shows the joint of a zinc plated aluminum bolt with a steel sheet with zinc-magnesium coating. The phases of the measuring points were categorized according to the ternary system Fe-Al-Zn at 330 °C. Additionally, they were classified according to the Al-Mg-Zn system at 335 °C (Figure 7). The measuring point EDX 01 consisted of over 94 at.-% Zn, which indicated a mixture of zinc mixed crystals and probably a small proportion of FeZn phases. The vertical section of the substance system at 95 at.-% zinc (no figure) indicated a mixture of $FeZn_{10}$, $FeZn_{13}$, and (Zn) at this measuring point.

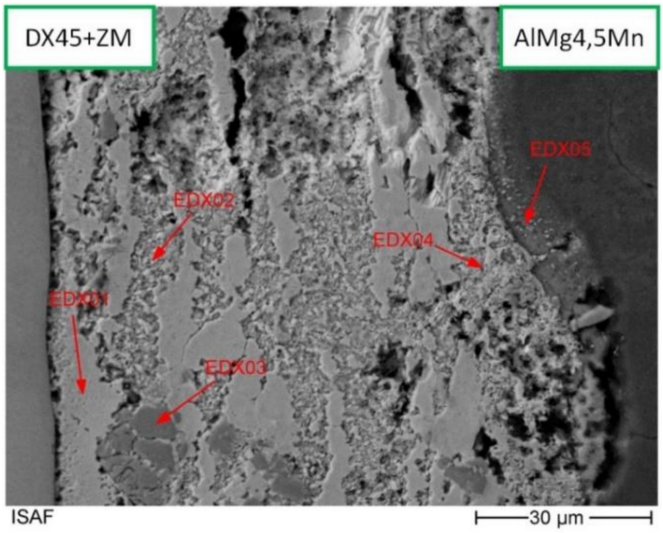

EDX-Point:	Fe (at.%)	Al (at.%)	Zn (at.%)	Mg (at.%)	Si (at.%)	Phases
01	2.49	0.45	94.91	0.44	1.72	(Zn)+$FeZn_{10}$+$FeZn_{13}$
02	2.56	6.95	87.18	1.01	2.67	(Al') + (Zn) + Fe_4Al_{13} or Mg_2Zn_{11} + (Zn) + (Al,Zn)
03	26.42	64.81	6.88	-	1.90	n. b.
04	-	6.58	83.08	1.18	9.16	$(Al)_2$ + (Si) + (Zn) or Mg_2Zn_{11} + (Zn) + (Al,Zn)
05	AlMg4.5Mn					

Figure 7. EDX analysis of the generated compound with magnesium in the zinc layer.

According to the isothermal cut of the system Al-Fe-Zn at 330 °C, the measuring point EDX 02 probably consisted of a mixture of (Al'), (Zn), and Fe_4Al_{13}. The measuring point EDX 03 could not be determined in this isothermal section. The classification of this point was conducted approximately according to the isothermal section of the ternary system Al-Fe-Zn at 450 °C. According to this, the composition at measuring point EDX 03 indicated the phase Fe_2Al_5.

The phase categorization of the determined compositions according to the Al-Zn-Mg ternary system (Figure 8) corresponded to a crystal mixture of Mg_2Zn_{11}, Zn-, and (Al, Zn) mixed crystals, as shown in Figure 7 [37]. The determination of EDX point 04 according to the ternary system Al-Mg-Zn also indicated a mixture of Mg_2Zn_{11}, Zn-, and (Al, Zn)- mixed crystals.

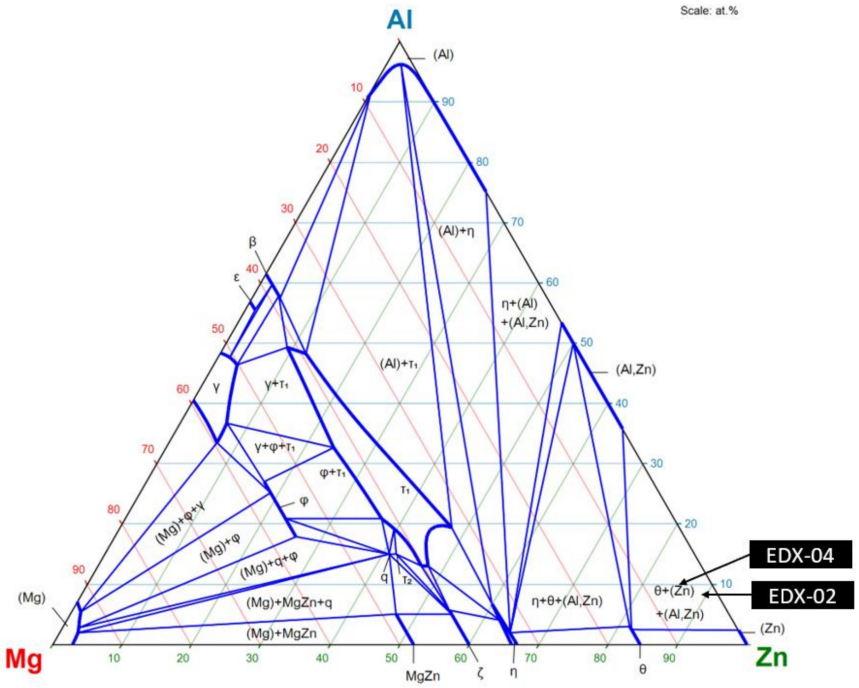

Figure 8. Isothermal section of the ternary system Al-Mg-Zn at 335 °C with EDX points [26].

Due to the relatively high Si content, the measuring point EDX 04 was additionally classified according to the isothermal section of the ternary system Al-Si-Zn at 300 °C [38]. At this point, the Al-Si-Zn system indicated a crystal mixture of Al, Si, and Zn mixed crystals, according to Figure 9.

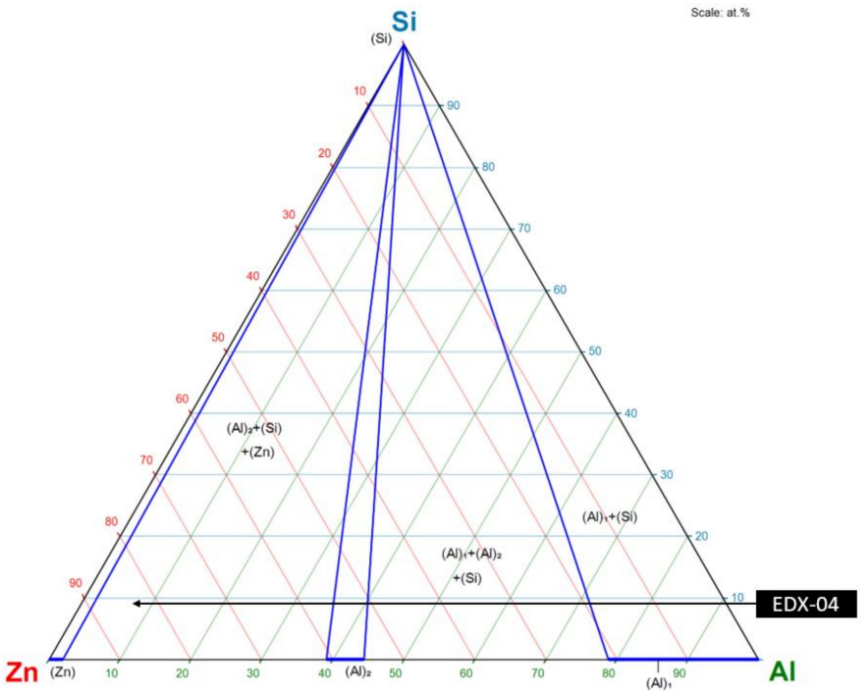

Figure 9. Isothermal section of the ternary system Al-Si-Zn at 300 °C with EDX point [27].

The intermediate layer of the compound in Figure 7 was largely composed of zinc mixed crystals and Fe-Zn phases. Brittle Fe_4Al_{13} phases also occurred. In addition to that, the Mg_2Zn_{11} phases, which are formed during the zinc coating of the steel sheets, were retained. Due to the upsetting

process shown in Figure 4, the intermediate phases appeared locally in the zinc layer, probably by diffusion bonding.

In the strain measurement, deformations of the sheet metal, the pin, and the joining zone were included. This was due to the test method, and allowed only tendentious statements about the deformability of the joining zone.

The influence of the different elements in the zinc layer is shown in tensile tests (Figure 10). The specimens were clamped in the fixture, as shown in Figure 11, with the geometry shown in Figure 1, to determine the strength values.

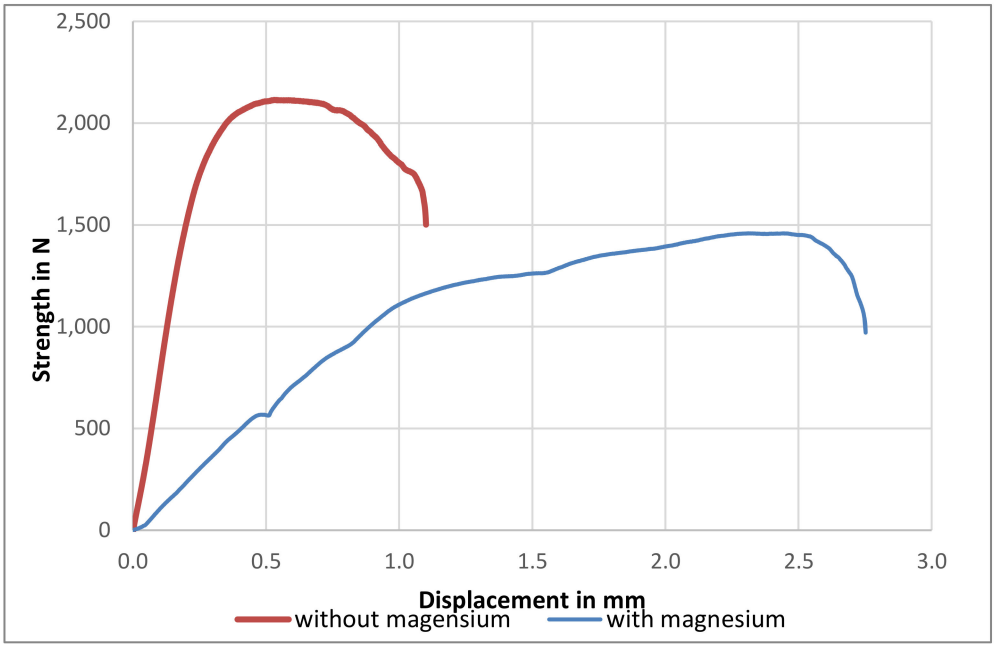

Figure 10. Strength and displacement curves for the dissimilar joints with zinc and zinc + magnesium layer on the steel sheets (exemplary).

Figure 11. clamping device for the determination of tensile strength values.

Since the exact reference surface could not be determined due to the strong plastic deformation, the force curves are given first. The change in displacement in the direction of tension is the reference value. The joint failed in the intermediate zinc layer [35]. For each state, three specimen were tested. The values in Figure 12 are the average values of three tests. The compound containing magnesium

showed a lower tensile strength. However, it also showed a considerably larger displacement in the tensile test. The strength of the joint with magnesium was only about 1500 N, while without magnesium a value of 2100 N was reached.

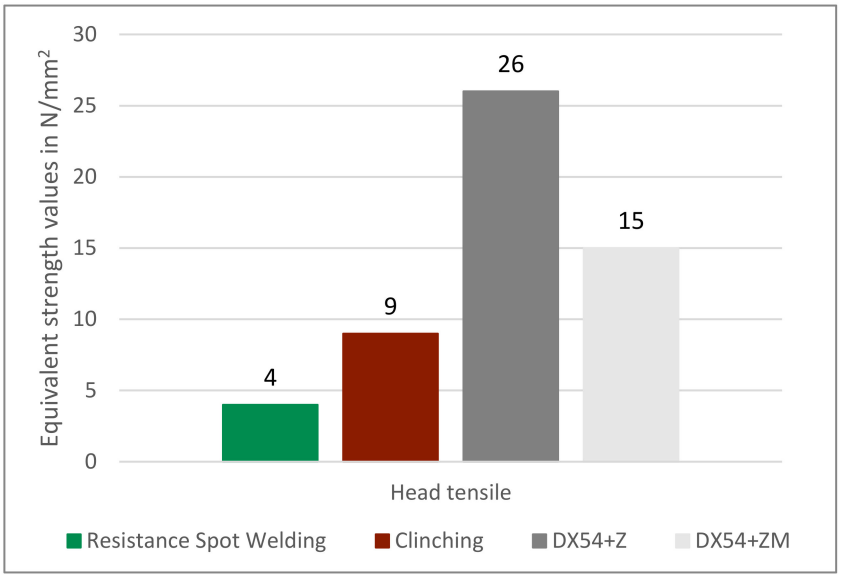

Figure 12. Equivalent strength values for resistance spot welding, clinching, and the shown joining processes.

The lower tensile strengths of the joints were probably due to the magnesium content of the zinc layer on the steel sheet, as the steel sheets used have the same thickness. The magnesium content of the zinc layer, therefore, changed the mechanical and technological properties on the one hand and influenced the formation of the firmly bonded joint on the other hand. Further investigations have to be carried out with a focus on this issue. [33].

For comparison of the strength values, resistance spot welding tests were carried out. Furthermore, the strength values of a clinch joint of the two base materials were determined. The comparison of the strengths of the hybrid composite forged joint with resistance spot welding and clinching was made possible, on the one hand by the high relevance of the two joining processes in industrial production, and on the other hand by the similar spot geometry of the joint. As a reference surface for the determination of the equivalent mechanical stresses at the different geometries, the load-bearing cross-sections were determined from the respective metallographic sections.

The resistance spot welding tests were carried out with an electrode force of 3 kN, a welding time of 200 ms and a welding current of 20 kA. Instead of AlMg4.5Mn studs, sheets of this material with a thickness of 1 mm were used. The steel sheet was on the cathode side and the aluminum sheet on the anode side during the joining process. During clinching, the aluminum sheet was arranged on the punch side and the steel sheet on the die side. Although the aluminum sheet was thicker than the steel sheet, this arrangement was chosen because the aluminum alloy was considerably softer than the steel grade. The tests were carried out with a clinching tool of the variant R-DF 8 without cutting portion. The residual bottom thickness of the samples was 0.8 mm and the undercut was approx. 0.7 mm. Figure 12 shows the results of tensile testing on different specimens for comparison. The highest tensile strength was achieved in the joints with an intermediate layer of zinc. The strength values for specimens with a zinc layer without magnesium content were the highest (26 N/mm^2) and the ones without magnesium were the second highest (15 N/mm^2). Resistance spot welding specimens showed the lowest strength values at 4 N/mm^2 [33], and were comparable with tensile strengths from the literature.

Although the dissimilar joint was generated in the solid state by applying pressure and high temperature, brittle intermetallic Fe-Al phases were formed. However, these were locally embedded in the zinc layer and did not form a continuous phase seam as described in other investigations. Furthermore, even a small amount of magnesium in the zinc layer on the steel sheet had a large influence on the mechanical and technological properties of the compound. However, it still needs to be clarified up to which extent the elements magnesium and silicon affect diffusion processes in the zinc interlayer, and further, the formation of the compound and intermetallic phases. Furthermore, the effect of the local deposition of brittle phases in contrast to the formation of a phase seam must be clarified. Further investigations must be carried out to clarify in detail the phase formation in the zinc intermediate layer during the joining process. This also includes an investigation of the concentration of the elements in the joining zone to clarify the diffusion conditions. Additionally, it is essential to identify the original composition of the zinc layers on the steel and aluminum, as well as the original phases. The conditions of diffusion and phase formation may be influenced by the presence of small amounts of silicon or eutectic MgZn-phases in the zinc-magnesium layer on the steel sheet [39,40]. For this purpose, further measurements are currently being carried out using EDX and XRD analysis.

In comparison to conventional processes, hybrid composite forging with a zinc intermediate layer offers a good alternative to the metallic continuity joining of steel-aluminum mixed joints. [32,33]. Contrary to assumptions, the temperature curves showed that the zinc layer did not melt during the joining process. Thus, the joint was probably created by superimposed diffusion welding. However, further investigations of the processes involved in material-to-material joining are still pending. Studies by Springer et al. showed an increasing amount of intermetallic phases in the joint was caused by zinc [41]. In contrast to this, results in literature regarding resistance spot welding have shown that zinc has prevented the formation of brittle intermetallic phases [17]. The positive effect of zinc on phase formation was reflected in the results presented in this paper. Despite the relatively short joining time, intermetallic phases were formed in the zinc layer of the joint by diffusion.

4. Conclusions

The results showed a clear influence of different zinc coatings on the strength of steel-aluminum mixed joints. The steel sheets were coated with different zinc layer compositions and joined with zinc plated aluminum bolts. For joining, the hybrid composite forging process was used. The forming process was superimposed by a diffusion process, which should be further investigated in detail. In this way, steel and aluminum could be joined. Hard and brittle intermetallic phases can hardly be avoided when steel and aluminum come into contact during a thermal joining process; however, by applying a zinc layer, the formation of the intermetallic phases could be limited to small local areas, which had a positive effect on the strength properties of the joint zone. Furthermore, tests under quasi-static load showed a significant influence of the alloying element magnesium in the zinc coating. Magnesium reduced the absolute strength by about a third.

The comparison of different zinc coatings showed that hybrid composite forging is a good alternative to the current state of joining technology to produce aluminum-steel mixed joints of point-like geometry. The results presented are currently being transferred into an actual forging process with higher forces and speeds by simulation and further trials. Furthermore, the influence of the chemical composition of the zinc layer on the aluminum specimens and the metallurgical processes in the joining zone during hybrid composite forging should be investigated in more detail.

This could allow the integration of the joining process into an industrial forming process as a new single step, whereby costs and throughput times can be reduced.

Author Contributions: Conceptualization, T.B. and K.T.; methodology, T.B.; validation, T.B., V.H., and K.T.; investigation, T.B. and V.H.; resources, V.W.; data curation, T.B., V.H., and K.T.; writing—original draft preparation, T.B. and V.H.; writing—review and editing, K.T. and V.W.; visualization, T.B. and V.H.; supervision, K.T. and V.W. All authors have read and agreed to the published version of the manuscript.

Funding: This research was funded by German Research Foundation.

Acknowledgments: Special thanks to the TU Clausthal for funding the Open Access publishing.

Conflicts of Interest: The authors declare no conflicts of interest. The funders had no role in the design of the study; in the collection, analyses, or interpretation of data; in the writing of the manuscript; or in the decision to publish the results.

References

1. Bian, J.; Zhu, Y.; Liu, X.-H.; Wang, G.-d. Development of Hot Dip Galvanized Steel Strip and Its Application in Automobile Industry. *J. Iron Steel Res. Int.* **2006**, *13*, 47–50. [CrossRef]
2. Radscheit, C.R. *Laserstrahlfügen von Aluminium mit Stahl*; BIAS-Verlag: Bremen, Germany, 1997.
3. Heumann, T.; Dittrich, S. Über die Kinetik der Reaktion von festem und flüssigem Aluminium mit Eisen. *Zeitschrift für Metallkunde* **1959**, *50*, 617–625.
4. Li, Y.; Liu, Y.; Yang, J. First principle calculations and mechanical properties of the intermetallic compounds in a laser welded steel/aluminum joint. *Opt. Laser Technol.* **2020**, *122*, 105875. [CrossRef]
5. Hoffmann, H.R. Über das Verhalten von Zink und Zink-Kupfer-Titan-Aluminium-Legierungen beim Kriechen unter hohen. Lasten. Dissertation, Technischen Universität Berlin, Berlin, Germany, 1971.
6. Goecke, S.-F. Energiereduziertes Lichtbogen-Fügeverfahren für Wärmeempfindliche Werkstoffe. In Proceedings of the Schweißen und Schneiden 2005—Vorträge der gleichnamigen Großen Schweißtechnischen Tagung, Essen, Germany, 12–14 September 2005; pp. 44–48.
7. Jank, N.; Staufer, H.; Bruckner, J. Schweißverbindungen von Stahl mit Aluminium—eine Perspektive für die Zukunft. *Berg Hüttenmännische Monatshefte* **2008**, *153*, 189–192. [CrossRef]
8. Yuce, C.; Karpat, F.; Yavuz, N. Investigations on the microstructure and mechanical properties of laser welded dissimilar galvanized steel–Aluminum joints. *Int. J. Adv. Manuf. Technol.* **2019**, *104*, 2693–2704. [CrossRef]
9. Goldmann, F.; Hahn, O.; Tetzlaff, U.; Kunze, S. Gefügemorphologie beim Widerstandspunktschweißen von Aluminium-Stahl-Verbindungen. *Schweißen Schneiden* **2015**, *67*, 238–244.
10. Leuschen, B. Beitrag zum Tragverhalten von Aluminium- und Aluminium/Stahl-Widerstandspunktschweissverbindungen bei Verschiedenartiger Beanspruchung. Ph.D. Thesis, RWTH, Fak. f. Maschinenwesen, Aachen, Germany, 1984.
11. Pereira, A.; Cabrinha, A.; Rocha, F.; Marques, P.; Fernandes, F.; Alves de Sousa, R. Dissimilar Metals Laser Welding between DP1000 Steel and Aluminum Alloy 1050. *Metals* **2019**, *9*, 102. [CrossRef]
12. Guan, Q.; Long, J.; Yu, P.; Jiang, S.; Huang, W.; Zhou, J. Effect of steel to aluminum laser welding parameters on mechanical properties of weld beads. *Opt. Laser Technol.* **2019**, *111*, 387–394. [CrossRef]
13. Lu, D.Q.; Cui, L.; Chen, H.X.; Chang, Y.Q.; Peng, Z.B.; He, D.Y. Laser-MIG Hybrid Keyhole Welded 6mm Steel/Aluminum Butt Joints. *Mater. Sci. Forum* **2019**, *944*, 581–592. [CrossRef]
14. Matsuda, T.; Adachi, H.; Sano, T.; Yoshida, R.; Hori, H.; Ono, S.; Hirose, A. High-frequency linear friction welding of aluminum alloys to stainless steel. *J. Mater. Process. Technol.* **2019**, *269*, 45–51. [CrossRef]
15. Mrzljak, S.; Gelinski, N.; Hülsbusch, D.; Schumacher, E.; Boehm, S.; Walther, F. Influence of Process Parameters, Surface Topography and Corrosion Condition on the Fatigue Behavior of Steel/Aluminum Hybrid Joints Produced by Magnetic Pulse Welding. *Key Eng. Mater.* **2019**, *809*, 197–202. [CrossRef]
16. Kashani, H.T.; Kah, P.; Martikainen, J. Laser Overlap Welding of Zinc-coated Steel on Aluminum Alloy. *Phys. Procedia* **2015**, *78*, 265–271. [CrossRef]
17. Köster, M.; Schuhmacher, B.; Sommer, D. The influence of the zinc content on the lattice constants and structure of the intermetallic compound Fe2Al5. *Steel Res.* **2001**, *72*, 371–375. [CrossRef]
18. Meco, S.; Ganguly, S.; Williams, S.; McPherson, N. Effect of Laser Processing Parameters on the Formation of Intermetallic Compounds in Fe-Al Dissimilar Welding. *J. Mater. Eng. Perform.* **2014**, *23*, 3361–3370. [CrossRef]
19. Elrefaey, A.; Gouda, M.; Takahashi, M.; Ikeuchi, K. Characterization of Aluminum/Steel Lap Joint by Friction Stir Welding. *J. Mater. Eng. Perform.* **2005**, *14*, 10–17. [CrossRef]
20. Eichhorn, F.; Emonts, M.; Leuschen, B. Widerstandspunktschweißen der Werkstoffkombination Alumnium-Stahl. *Schweißen Schneiden* **1982**, *34*, 15–20.
21. Ozaki, H.; Kutsuna, M. Laser-roll welding of a dissimilar metal joint of low carbon steel to aluminium alloy using 2 kW fibre laser. *Weld. Int.* **2009**, *23*, 345–352. [CrossRef]

22. Ozaki, H.; Kutsuna, M. Dissimilar Metal Joining of Zinc Coated Steel and Aluminum Alloy by Laser Roll Welding. In *Welding Processes*; Kovacevic, R., Ed.; InTech: London, UK, 2012; ISBN 978-953-51-0854-2.
23. Pardal, G.; Meco, S.; Ganguly, S.; Williams, S.; Prangnell, P. Dissimilar metal laser spot joining of steel to aluminium in conduction mode. *Int. J. Adv. Manuf. Technol.* **2014**, *73*, 365–373. [CrossRef]
24. Engelbrecht, L.; Meier, O.; Ostendorf, A.; Haferkamp, H. Einflüsse auf die mechanischen Eigenschaften lasergelöteter Mischverbindungen aus Stahl und Aluminium. *Materialwissenschaft Werkstofftechnik* **2006**, *37*, 272–278. [CrossRef]
25. Girard, M.; Huneau, B.; Genevois, C.; Sauvage, X.; Racineux, G. Friction stir diffusion bonding of dissimilar metals. *Sci. Technol. Weld. Join.* **2013**, *15*, 661–665. [CrossRef]
26. Meco, S.; Cozzolino, L.; Ganguly, S.; Williams, S.; McPherson, N. Laser welding of steel to aluminium: Thermal modelling and joint strength analysis. *J. Mater. Process. Technol.* **2017**, *247*, 121–133. [CrossRef]
27. Langner, J.; Stonis, M.; Behrens, B.-A. Hybridschmieden eines Druckflansches. Available online: https://www.umformtechnik.net/binary_data/3165637_hybridschmieden-langner.pdf (accessed on 9 January 2020).
28. Behrens, B.-A.; Kosch, K.-G. Influence of different alloying elements on the intermetallic phase seam thickness of compound forged steel-aluminum parts. *Prod. Eng. Res. Dev.* **2011**, *5*, 517–522. [CrossRef]
29. Behrens, B.-A.; Odening, D.; Holz, F.; Kosch, K.-G. Finite Elemente Modellierung der induktiven Erwärmung hybrider Stahl-Aluminium Bauteile. Available online: https://www.umformtechnik.net/binary_data/99892_fem_erw_rmung_ifum_kosch.pdf (accessed on 6 January 2020).
30. Behrens, B.-A.; Kosch, K.-G. Development of the heating and forming strategy in compound forging of hybrid steel-aluminum parts. *Materialwissenschaft Werkstofftechnik* **2011**, *42*, 973–978. [CrossRef]
31. Behrens, B.-A.; Holz, F. Verbundschmieden hybrider Stahl-Aluminium Bauteile. *Materialwissenschaft Werkstofftechnik* **2008**, *39*, 599–603. [CrossRef]
32. Bick, T. *Hybrides Verbundschmieden von Aluminium und Stahl durch Bildung einer Zinkzwischenschicht: Bestimmung der Prozesseinflussgrößen und Verbindungseigenschaften. Masterarbeit*; Technische Universität Clausthal: Clausthal, Germany, 2018.
33. Bick, T.; Treutler, K.; Wesling, V. *Charakterisierung der Verbindungseigenschaften hybrid verbundgeschmiedeter Stahl Aluminium Mischverbindungen in Abhängigkeit der Zinkschichtzusammensetzungen*; Assistentenseminar Füge- und Schweißtechnik No. 39; DVS Media: Düsseldorf, Germany, 2019.
34. Hoppe, C.; Ebbert, C.; Grothe, R.; Schmidt, H.C.; Hordych, I.; Homberg, W.; Maier, H.J.; Grundmeier, G. Influence of the Surface and Heat Treatment on the Bond Strength of Galvanized Steel/Aluminum Composites Joined by Plastic Deformation. *Adv. Eng. Mater.* **2016**, *18*, 1371–1380. [CrossRef]
35. Bick, T.; Treutler, K.; Wesling, V. *Soldering of Steel Sheets and Zinc Coated Aluminum by Hybrid Composite Forging*; 2018.
36. Ghosh, G. Al-Fe-Zn Ternary Phase Diagram Evaluation. Available online: http://www.msi-eureka.com/full-html/10.17658.3.6/Al-Fe-Zn_Ternary_Phase_Diagram_Evaluation/ (accessed on 20 August 2019).
37. Petrov, D.; Watson, A.; Gröbner, J.; Rogl, P.; Tedenac, J.; Bulanova, M.; Turkevich, V.; Lukas, H. Al-Mg-Zn Ternary Phase Diagram Evaluation. Available online: http://www.msi-eureka.com/full-html/10.11491.3.7/Al-Mg-Zn_Ternary_Phase_Diagram_Evaluation/ (accessed on 28 January 2020).
38. Suzuki, T. Al-Si-Zn Ternary Phase Diagram Evaluation. Available online: http://www.msi-eureka.com/full-html/10.14605.1.6/Al-Si-Zn_Ternary_Phase_Diagram_Evaluation/ (accessed on 29 January 2020).
39. Silvayeh, Z.; Vallant, R.; Sommitsch, C.; Götzinger, B.; Karner, W.; Hartmann, M. Influence of Filler Alloy Composition and Process Parameters on the Intermetallic Layer Thickness in Single-Sided Cold Metal Transfer Welding of Aluminum-Steel Blanks. *Metall. Mater. Trans. A* **2017**, *48*, 5376–5386. [CrossRef]
40. Schuerz, S.; Fleischanderl, M.; Luckeneder, G.H.; Preis, K.; Haunschmied, T.; Mori, G.; Kneissl, A.C. Corrosion behaviour of Zn–Al–Mg coated steel sheet in sodium chloride-containing environment. *Corros. Sci.* **2009**, *51*, 2355–2363. [CrossRef]
41. Springer, H.; Szczepaniak, A.; Raabe, D. On the role of zinc on the formation and growth of intermetallic phases during interdiffusion between steel and aluminium alloys. *Acta Mater.* **2015**, *96*, 203–211. [CrossRef]